# Cryogenic cyclical etching of Si using CF_4 plasma passivation steps: The role of CF radicals

Jack Nos, Sylvain Iséni, Martin Kogelschatz, Gilles Cunge, Philippe Lefaucheux, Rémi Dussart, Thomas Tillocher, Émilie Despiau-Pujo

# Cryogenic cyclical etching of Si using $CF_4$ plasma passivation steps: The role of CF radicals Ⓕ

Jack Nos,[1,a] Sylvain Iséni,[1] Martin Kogelschatz,[2] Gilles Cunge,[2] Philippe Lefaucheux,[1] Rémi Dussart,[1] Thomas Tillocher,[1] and Émilie Despiau-Pujo[2]

**AFFILIATIONS**

[1]GREMI, Orléans University-CNRS, 14 Rue d'Issoudun BP 6744, 45067 Orléans, France
[2]University Grenoble Alpes, CNRS, CEA/LETI-Minatec, Grenoble INP, LTM, Grenoble F-38054, France

[a]Author to whom correspondence should be addressed: jack.nos@univ-orleans.fr

**ABSTRACT**

Ultraviolet (UV) absorption spectroscopy is used to monitor the CF radical density in $CF_4$ inductively coupled plasma (ICP) plasmas as a function of the substrate temperature. The CF density decreases dramatically when the wafer temperature is reduced from 20 to $-130\,°C$ by applying identical plasma conditions, demonstrating that the CF surface sticking coefficient increases as the surface temperature is reduced. This suggests that $CF_4$ plasma could be used to form sidewall passivation layers and perform anisotropic etching at cryogenic temperature, which is impossible at room temperature. Subsequently, a cyclical Bosch type etching process of silicon was evaluated at $-100\,°C$ using $CF_4$ plasma to passivate the trench sidewalls. Anisotropic etch profiles were obtained with an etch rate of $4.4\,\mu m/min$. Compared to a typical Bosch process using highly polymerizing $c\text{-}C_4F_8$ plasma, chamber wall contamination could be significantly reduced, alleviating a major issue of this cyclic process. Furthermore, $CF_4$ has a 28% lower global warming potential than $c\text{-}C_4F_8$.

In most plasma etching processes, the etching anisotropy relies on the formation of protecting passivation layers on the feature sidewalls. These layers are formed by the deposition of plasma radicals and prevent the sidewalls from lateral etching. Their formation and control are considered as a challenge in high aspect ratio feature etching (such as silicon trenches). Furthermore, due to the necessity to form passivation layers, most fluorocarbon plasma conditions are such that the plasma tends to deposit "polymer" on all the surfaces that are not bombarded by energetic ions. For instance, polymer deposition on the reactor walls is known to be a serious issue for process reproducibility and defectivity (particles flake off).[1–6] Reactor cleaning treatments between each processed wafer are typically used to minimize these issues but reduce the reactor throughput and have a significant cost (both financially and environmentally). Deep silicon etching of high aspect ratio features is important in many applications such as TSV, MEMS, or DRAM devices fabrication.[7–12] It has been carried out by using the so-called Bosch process for 30 years. This process consists of a cyclic repetition of an etching step using $SF_6$ plasma followed by a fluorocarbon plasma step to passivate the trench sidewalls and ensure the etching anisotropy. It is more robust than the standard cryoetching process, which uses a continuous $SF_6/O_2$ plasma to produce smooth sidewalls through $SiO_xF_y$ passivation at around $-100\,°C$.

This technique was developed by Laermer and Schilp[7] who evaluated different fluorocarbon gases for their ability to passivate silicon at ambient temperature.[7] It resulted that $c\text{-}C_4F_8$ was the best candidate out of a list including also $CHF_3$, $C_2H_2F_2$, $C_3F_6$, $C_4F_6$, and $C_4F_{10}$.[8] Since then, almost all processes developed with this technique include $c\text{-}C_4F_8$ as a passivation gas and are performed at ambient temperature.[9–12] However, a major drawback when using these fluorocarbon gases in high density plasmas is the rapid contamination of the chamber walls with the formation of a thick fluorocarbon polymer layer. The high polymer deposition rate is due to the low F/C ratio of the parent gas and/or to the presence of hydrogen that scavenges fluorine atoms from the plasma by forming HF. As a result, there are not enough fluorine atoms available in the plasma to etch back the carbon that deposits continuously on the reactor walls in the form of $C_xF_y$ radicals and ions.[13–15]

By contrast, $CF_4$ plasmas tend to be deposition free owing to the high F/C ratio in the parent gas: the fluorocarbon species that deposit on the surfaces are rapidly captured back in the plasma in the form of $CF_2$ or $CF_4$ volatile etch products. The high density of F atoms generated in $CF_4$ plasmas is, thus, useful to prevent polymer formation on the reactor walls, which stay clean or only get weakly contaminated. It also leads to faster etch rates at room temperature.[16–18] However, this

is at the detriment of the etching anisotropy since no sidewall passivation layer is formed to prevent lateral etching in this chemistry. $CF_4$ can be combined with other gas compounds such as $H_2$ or $NH_3$, as it was reported for thin-film deposition or surface modification in ALE applications,[19,20] but it would again result in $C_xH_yF_z$ deposition on the reactor walls. It shall be underlined that most papers reporting on plasma surface interactions in $CF_4$ plasmas deal with experiments that were carried out at room temperature. However, it is well known that the decrease in substrate temperature can enhance fluorocarbon condensation and passivation reactions. For $c$-$C_4F_8$, several studies showed that a lower substrate temperature leads to thicker fluorocarbon passivation layers under otherwise identical plasma etching conditions.[21,22] However, there are no detailed studies reporting on the impact of surface temperature on the shift of the polymerization/etching equilibrium of fluorocarbon plasma processes. In particular, the sticking coefficient of several reactive species including $CF_x$ radicals was shown to increase when the surface temperature is reduced,[1,23,24] but the impact of surface temperature on the $CF_x$ layer formation was not investigated. The purpose of this study is to evaluate the impact of substrate temperature on the density of CF and $CF_2$ radicals in a $CF_4$ high density plasma process. These two radicals are detected by broadband ultraviolet (UV) absorption spectroscopy (UVAS).[25–29] Based on our observations, we will, in a second step, discuss the development of a Bosch type process using $CF_4$ as a passivation gas at $-100\,°C$.

The experiments were performed using an Oxford Instruments Plasma Pro 100 Cobra inductively coupled plasma (ICP) reactor, which disposes of a mechanical clamping cryogenic chuck cooled with liquid nitrogen, as described in Ref. 21. UVAS measurements were realized under the same $CF_4$ plasma conditions but with two different chuck temperatures of $20\,°C$ and $-130\,°C$. The removal of the wafer clamping crown was necessary to prevent the optical beam vignetting by the chuck. As a result, the acquisitions were performed using a 150 mm diameter Si wafer, which was fixed to the chuck using the kapton tape. Every acquisition was preceded by an $O_2$ plasma process to clean the ICP chamber and to remove any fluorocarbon layer that would have formed on the Si substrate during the previous experiment. A helium backing pressure of 500 Pa was fixed during the process tests to allow thermal transfer between the chuck and the substrate. The UVAS measurements were performed using a Hamamatsu Energetiq ED-99X-FC-S laser-driven light source ($LDLS^{TM}$) and a Princeton Instruments Acton Spectra Pro SP 2750 750 mm triple grating imaging spectrometer equipped with a Pylon-400B CCD detector.[30–32] The light signal was collimated and passed through the ICP reactor at a vertical distance of 1.25 cm above the substrate holder inside the chamber. At this level, the reactor diameter is equal to 38.0 cm. However, two external vacuum tubes with a diameter of 1 cm and a total length of 25 cm were added to the reactor openings to limit fluorocarbon plasma deposition, thus transmission variations on the quartz windows. The total optical path is, thus, of 63 cm. Absorption spectroscopy acquisitions were performed in a pure $CF_4$ plasma (50 sccm; Chamber pressure: 4.0 Pa; ICP Power: 1500 W; No bias power). The acquisitions were launched once the reflected ICP minimal power reached a stable minimal value. Figures 1 (a) and 1(b) show the transmission spectra obtained, respectively, in the CF and $CF_2$ radical absorbance regions. In each case, the UV absorption spectra were acquired for two different substrate temperatures of $-130$ and $20\,°C$ under otherwise identical plasma conditions. These absorbance spectra $A$ were obtained from 4 separate measurements and are

related to the absorption path L, absorption cross section $\sigma$, and absorbing species density n through the Beer-Lambert law [Eq. (1)]:

$$-ln\left(\frac{I_{LP} - I_P}{I_L - I_{BG}}\right) = -ln\left(\frac{I_T}{I_0}\right) = A = \sigma \cdot n \cdot L, \quad (1)$$

where $I_{LP}$ is the signal acquired with both the lamp and the plasma ON, $I_P$ is the plasma emission measured with the lamp OFF (using a shutter), $I_L$ is the lamp signal measured with the plasma OFF, and $I_{BG}$ is the background measured with the lamp and the plasma OFF. By integrating Eq. (1) over an entire rovibronic transition [Eq. (2)], one can then deduce the absolute density n of the absorbing species knowing the oscillator strength $f_{v'v''}$,

$$\int \frac{I_0 - I_T}{I_0} \cdot d\lambda = 8.85 \times 10^{-20} \lambda_0^2 \cdot f_{v'v''} \cdot n \cdot L. \quad (2)$$

According to Luque et al.,[26] for the CF A-X[1,0] transition around $\lambda_0 = 223.9$ nm shown in Fig. 1(a), the value of the oscillator strength $f_{v'v''}$ is $4.76 \times 10^{-3}$. Since CF is reactive on surfaces,[13] we assumed that its density rapidly drops inside the high aspect ratio tubes that separate the plasma chamber from the UV windows, and we, thus, consider an absorption path of $L = 38\,cm$, which corresponds to the reactor diameter. The integrated absorbance between 222 and 224.5 nm is $8.0 \times 10^{-3}$, leading to an absolute CF density of about $n = 1.0 \times 10^{13}$ cm$^{-3}$ at $20\,°C$. At $-130\,°C$, the integrated absorbance is $4.86 \times 10^{-3}$ and $n = 6 \times 10^{12}$ cm$^{-3}$. Therefore, the substrate cooling has a significant impact on the CF radical density in the plasma near the wafer surface level as it drops by roughly 40% at $-130\,°C$.

By contrast, Fig. 1(b) shows that the absorption spectrum of the $CF_2$ A-X is almost independent of the substrate temperature. For the determination of $CF_2$ radical absolute density, we used the cross section reported by Sharpe et al.[33] and later analyzed into more detail by Bulcourt et al.,[28] which is $\sigma = 2.91 \times 10^{-17}$ cm$^2$ at 249.0 nm. Considering the fact that $CF_2$ does not stick on surfaces, an absorption path of 63 cm was chosen (reactor diameter + optical tubes). It leads to a $CF_2$ density of $1.70 \times 10^{13}$ cm$^{-3}$, which is almost independent of the substrate temperature. Indeed, only minor differences are observed in the two spectra measured at $20\,°C$ and $-130\,°C$. They can be attributed to a small uncertainty on the baseline of this wideband absorption spectrum caused by fluctuation of the lamp source emission spectrum.[34] The only significant difference is a slightly higher absorption at $20\,°C$ around 259.46, 262.8, and 266.3 nm, which corresponds to absorption from the first populated vibrational level of $CF_2$ (A(0,v',0) ← X(0,1,0)). It is beyond the scope of this paper to discuss this observation, but since $CF_2$ is partly produced on surfaces, it suggests that a cold surface reduces the production of vibrationally excited $CF_2$.

The absolute values of the CF and $CF_2$ density measured under our conditions are very close to those deduced by Booth et al.[25] under similar plasma conditions ($CF_4$ ICP plasma at 30 mTorr) applied on a substrate at room temperature. The striking feature in our result is that the substrate temperature has a significant impact on the CF radical density but not on the $CF_2$ radical density. This correlates with the well-known fact that CF sticks on surfaces, while $CF_2$ is typically produced by surfaces (by carbon etching reaction and ion neutralization).[13,15]

From in situ ellipsometric measurement realized on the sticked 6″ Si wafer using the modeling conditions detailed in Ref. 21, we observe $CF_x$ polymer deposition on the wafer at a rate of about
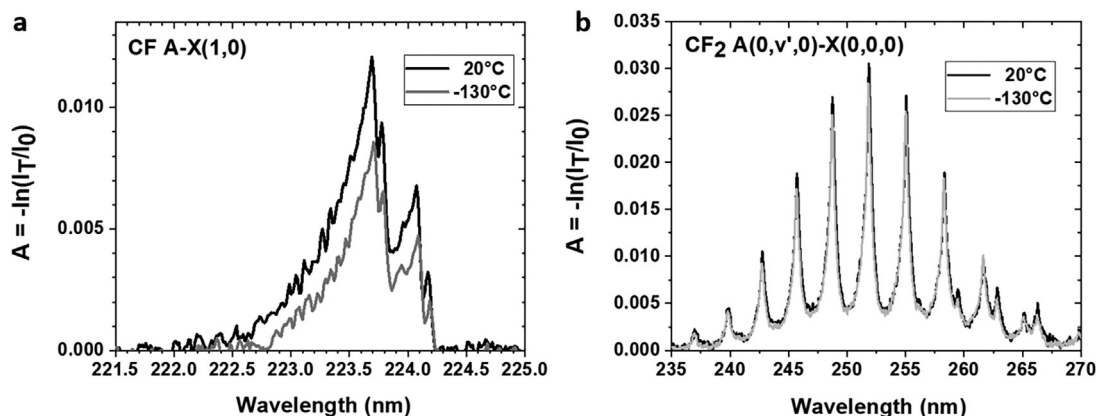
**FIG. 1.** Absorption spectra measured in a $CF_4$ plasma (50 sccm, 4 Pa, 1.5 kW ICP power, no bias power) for chuck temperatures of 20 °C and −130 °C. (a) $A\,^2\Sigma \leftarrow X\,^2\Pi$ (1,0) transition of CF and (b) A(0, v, 0) ← X(0, 0, 0) transition of $CF_2$.

2.6 nm s$^{-1}$ at −130 °C, yet no polymer accumulation is detected at 20 °C. In heavily dissociated ICP fluorocarbon plasmas, the polymer precursors are expected to be C, CF, and $C_xF_y^+$ ions. The thermal flux of CF (assuming a gas temperature of 450 K near the surface) is about $1.0 \times 10^{17}$ cm$^{-2}$.s$^{-1}$ and is one order of magnitude higher than the ion flux. Since the carbon atom density is not expected to be high, CF is, thus, expected to be the main precursor of $CF_x$ film formation at low temperature. Indeed, by considering that the cold wafer area is small compared to the total chamber wall surfaces (which stay at room temperature), the observation of a 40% drop in the CF density when the substrate is cooled from room temperature to −130 °C implies that the surface loss rate of CF radicals increases strongly at low temperature, and that CF participates significantly to polymer deposition on cold surfaces. It remains difficult to estimate a true CF surface sticking probability from our data because the net $CF_x$ polymer deposition rate measured by ellipsometry results from a deposition/etching competition: a significant part of CF radicals that are lost by sticking at the surface do not stay there but are recycled in the plasma in the form of $CF_2$ and $CF_4$ volatile products following $CF_x$ polymer ion-enhanced etching by F atoms. Nevertheless, by neglecting this important etching component, we can provide a rough estimation of the CF surface loss probability: we need a 10% sticking probability to explain the measured deposition rate [assuming a film density around 2 g.cm$^{-3}$ (Ref. 35)]. This sticking probability is already quite high, and as discussed earlier, it is probably underestimated since the film etching by F atoms is not considered in the calculation. We, thus, concluded that CF radicals play a major role in polymer film formation on cold surfaces.

Following the observation that $CF_4$ plasma shifts to a polymerizing regime on low temperature surfaces, it was decided to evaluate the feasibility of using pure $CF_4$ plasmas to etch silicon anisotropically at cryogenic temperatures by implementing a Bosch type process. As a starting point, we simply replaced c-$C_4F_8$ by $CF_4$ in a Bosch process, which was studied at −100 °C in Ref. 21. No intermediate steps were placed between the passivation and etching steps. The exact process parameters that were tested are listed in Table I. To evaluate the process etching anisotropy, we used $3 \times 3$ cm$^2$ Si samples with a patterned 1.2 μm thick $SiO_2$ hard-mask. The mask consists of an array of trenches with different width openings ranging from 2 to 10 μm. The

samples were glued on $SiO_2$ 4″ carrier wafers using a specific thermal glue. A helium backing pressure of 1300 Pa was fixed during the etching tests (where the clamping crown removed for UVAS was reinstalled). A thermalization period of 5 min was fixed for the etching tests realized at −100 °C to enable the substrate to cooldown. The chamber pressure for etching and passivation steps was fixed using an automatic pressure controller (APC) rotating valve. A limit of 200 etching/deposition cycles was set in order to obtain significantly deep features, which could be compared to each other by scanning electron microscopy (SEM) (using a Zeiss SUPRA 40). The etch profiles obtained on 6.0 μm wide trenches are shown in Fig. 2 at 20 °C (2.a) and at −100 °C (2.b). A closer view of the etch profile obtained at −100 °C near the mask area is shown in Fig. 2(c).

It is observed that $CF_4$ plasma sidewall passivation is considerably enhanced at −100 °C. Indeed, isotropic etch profiles are observed at room temperature [Fig. 2(a)], whereas quasi-anisotropic etch profiles were obtained at −100 °C under the same plasma conditions [Fig. 2(b)] with aspect ratios ranging from roughly 26:1 to 8:1. The etch profiles are slightly negative but with a constant angle, which suggests no gradual alteration of the etching/deposition equilibrium throughout the process. An etch rate of approximately 4.4 μm/min was determined in Fig. 2(b), which corresponds to the etch rates that were observed when using c-$C_4F_8$ gas in similar process conditions.[21] Scalloping marks are observed in Fig. 2(c), which are testimony of an adequate fluorocarbon passivation in these process conditions. By considering the amount of $SiO_2$ hard-mask that was etched during the process, a Si:$SiO_2$ etching selectivity of roughly 80:1 is evaluated.

Complementary tests were realized on a $SiO_2$ blanket sample glued on a 4″ Si wafer carrier. With the same plasma process parameters as those applied during the UVAS experiments (50 sccm $CF_4$, 4 Pa, 1500 W ICP power, no bias power), using this time a helium backing pressure of 1300 Pa, a fluorocarbon layer deposits at a rate of roughly 360 nm/min at −130 °C, which was characterized both by SEM and in situ ellipsometry. Subsequently, by applying the same $CF_4$ plasma process, this time at ambient temperature, the $CF_x$ layer is removed from the sample at a rate of approximately 37 nm/min, before etching the $SiO_2$ layer at a rate of roughly 4 nm/min. These results demonstrate that no fluorocarbon contamination of the

TABLE I. Set of $CF_4/SF_6$ Bosch process parameters tested to study the impact of substrate temperature on the etch profiles.

| Temperature (°C) | +20 °C or −100 °C | |
|---|---|---|
| Process duration | 200 Bosch cycles (16 min 40 s) | |
| Process step | Etching step | Passivation step |
| Gas | $SF_6$ | $CF_4$ |
| Flow (sccm) | 300 sccm | 20 sccm |
| Step time (s) | 3 s | 2 s |
| Pressure (Pa) | ≈3.0 Pa | ≈1.0 Pa |
| Source power (W) | 1500 W | 1500 W |
| Bias power (W)/Bias voltage measured on a Si wafer (V) | 15 W/≈135 V | 15 W/≈65 V |

chamber walls should result from the application of this process at low substrate temperatures.

In conclusion, our results show that the substrate temperature, if it can be reduced to cryogenic range, allows us to induce a transition from Si etching by F atoms at ambient temperature to $CF_x$ polymer deposition at low temperature when applying a $CF_4$ plasma process. This effect is attributed (at least partly) to a large increase in the surface sticking probability of CF radicals on the cold wafer surface. Since the feature sidewalls are not bombarded by ions, and $CF_2$ sticking probability does not increase at low temperature, it is expected that CF radicals (and possibly C atoms) play a major role in the passivation layer formation at cryogenic temperatures. It is also expected that the net deposition rate of $CF_x$ polymer (which results from an etching/deposition competition) is increasing because the $CF_x$ film chemical etching rate by F atoms should also drop when the temperature is decreased.

In terms of plasma processing, our results have important implications. The first obvious one is the possibility to design Bosch like processes in which c-$C_4F_8$ is replaced by $CF_4$. This should alleviate a major issue of the Bosch process: the contamination of the chamber walls by heavy deposition of $CF_x$ film, which is a major concern in terms of process throughput and reproducibility. Indeed, from our results, the $CF_4$ plasma is not expected to deposit any polymer on the reactor surfaces, which are at room temperature. Furthermore, $CF_4$ has a 28% lower

GWP than c-$C_4F_8$.[36,37] Additional optimization is needed to ameliorate the anisotropy of etch profiles at −100 °C. Possible solutions include the increase in the passivation step duration and/or decrease in the etch step duration. Contrarily to the standard cryoetching process, our results give hope that similar etch profiles could be obtained using $CF_4$ fluorocarbon passivation at intermediate substrate temperatures, where chillers could replace liquid nitrogen-based cooling systems.

More generally, this work suggests that the reduction of substrate temperature offers numerous processing opportunities due to enhanced passivation reactions with the cooled substrate. It may contribute to reduce the consumption of necessary gases for a variety of processes. In this case, it also shows that process gases that are not suitable at ambient temperature may be used at cooler temperatures to obtain similar etch results. This opens up interesting perspectives toward cost reduction and environmental compliance solutions.

## AUTHOR DECLARATIONS
### Conflict of Interest

The authors have no conflicts to disclose.

### Author Contributions

**Jack Nos:** Conceptualization (equal); Data curation (equal); Formal analysis (equal); Investigation (equal); Methodology (equal); Software (equal); Supervision (equal); Validation (equal); Visualization (equal); Writing – original draft (equal); Writing – review & editing (equal). **Sylvain Iséni:** Conceptualization (equal); Data curation (equal); Formal analysis (equal); Investigation (equal); Methodology (equal); Resources (equal); Software (equal); Supervision (equal); Validation (equal); Visualization (equal); Writing – review & editing (equal). **Martin Kogelschatz:** Conceptualization (equal); Data curation (equal); Formal analysis (equal);
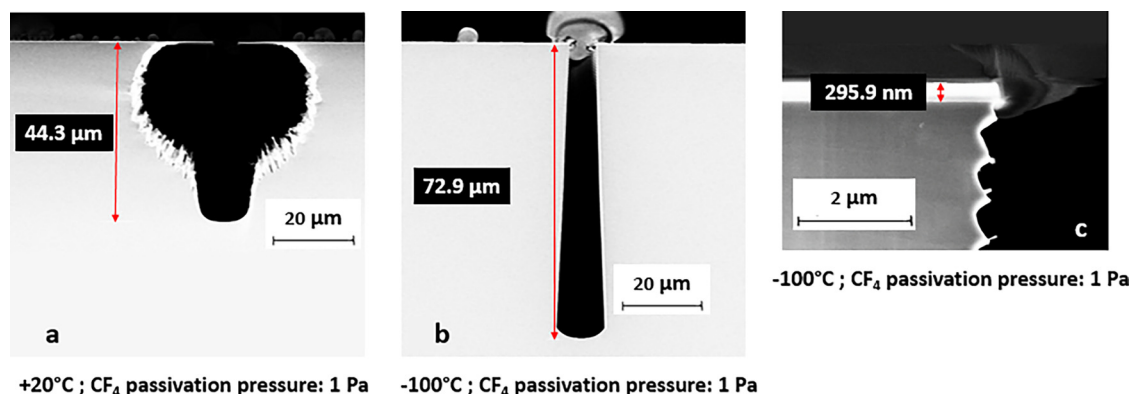
FIG. 2. Etch profiles obtained with a $CF_4/SF_6$ Bosch process at +20 °C and −100 °C (6 $\mu$m wide trenches); process conditions listed in Table I.

Investigation (equal); Methodology (equal); Software (equal); Supervision (equal); Validation (equal); Visualization (equal); Writing – review & editing (equal). **Gilles Cunge:** Conceptualization (equal); Data curation (equal); Formal analysis (equal); Investigation (equal); Methodology (equal); Software (equal); Supervision (equal); Validation (equal); Visualization (equal); Writing – review & editing (equal). **Philippe Lefaucheux:** Conceptualization (equal); Investigation (equal); Methodology (equal); Resources (equal); Software (equal); Supervision (equal); Validation (equal); Visualization (equal); Writing – review & editing (equal). **Rémi Dussart:** Conceptualization (equal); Formal analysis (equal); Funding acquisition (equal); Investigation (equal); Methodology (equal); Project administration (equal); Resources (equal); Supervision (equal); Validation (equal); Visualization (equal); Writing – review & editing (equal). **Thomas Tillocher:** Conceptualization (equal); Formal analysis (equal); Funding acquisition (equal); Investigation (equal); Methodology (equal); Project administration (equal); Resources (equal); Supervision (equal); Validation (equal); Visualization (equal); Writing – review & editing (equal). **Émilie Despiau-Pujo:** Conceptualization (equal); Formal analysis (equal); Funding acquisition (equal); Investigation (equal); Methodology (equal); Project administration (equal); Resources (equal); Supervision (equal); Validation (equal); Visualization (equal); Writing – review & editing (equal).

## DATA AVAILABILITY

The data that support the findings of this study are available within the article.

## REFERENCES

[1] M. Schaepkens, R. C. M. Bosch, T. E. F. M. Standaert, G. S. Oehrlein, and J. M. Cook, "Influence of reactor wall conditions on etch processes in inductively coupled fluorocarbon plasmas," J. Vac. Sci. Technol., A **16**, 2099–2107 (1998).

[2] S. McColman, *Advanced Bosch Processing on the Oxford Plasmalab ICPRIE* (NanoFab, University of Alberta, 2009), available at https://www.nanofab.ualberta.ca/wp-content/uploads/2009/05/bosch_advanced.pdf.

[3] C.-Y. Lee and A. Shen, "Residual polymer effect on shallow trench Bosch process stability," AIP Adv. **10**, 075311 (2020).

[4] M. Puech, "Heating jacket plasma etching reactor, etching method using same," U.S. patent 20050224178A1 (13 October 2005).

[5] W. S. Kennedy, R. A. Maraschin, and T. E. Wicker, "Semiconductor processing equipment having radiant heated ceramic liner," U.S. patent WO 01/22478 A1 (29 March 2001).

[6] B. A. Cruden, S. P. Sharma, M. Meyyappan, and V. V. S. Rao, "Detection of chamber conditioning by $CF_4$ plasmas in an inductively coupled plasma reactor," J. Vac. Sci. Technol., B **20**, 353 (2002).

[7] F. Laermer and A. Schilp, "Method anisotropic plasma etching substrates," U.S. patent 5498312A (12 March 1996).

[8] F. Laermer and A. Urban, "Through-silicon vias using bosch DRIE process technology," in *Ultra-Thin Chip Technology and Applications, Joachim Burghartz* (Springer, New York, NY, 2010), pp. 81–91.

[9] B. Wu, A. Kumar, and S. Pamarthy, "High aspect ratio silicon etch: A review," J. Appl. Phys. **108**, 051101 (2010).

[10] S. L. Burkett, M. B. Jordan, R. P. Schmitt, L. A. Menk, and A. E. Hollowell, "Tutorial on forming through-silicon vias," J. Vac. Sci. Technol. A **38**, 031202 (2020).

[11] O. Fursenko, J. Bauer, S. Marschmeyer, and H.-P. Stoll, "Through silicon via profile metrology of Bosch etching process based on spectroscopic reflectometry," Microelectron. Eng. **139**, 70 (2015).

[12] M. A. Blauw, T. Zijlstra, and E. van der Drift, "Balancing the etching and passivation in time-multiplexed deep dry etching of silicon," J. Vac. Sci. Technol., B **19**, 2930–2934 (2001).

[13] G. Cunge and J. P. Booth, "$CF_2$ production and loss mechanisms in fluorocarbon discharges: Fluorine-poor conditions and polymerization," J. Appl. Phys. **85**, 3952 (1999).

[14] J. P. Booth and G. Cunge, "CFx radical creation and destruction at surfaces in fluorocarbon plasmas," J. Plasma Fusion Res. **75**, 821 (1999).

[15] W. Schwarzenbach, G. Cunge, and J. P. Booth, "High mass positive ions and molecules in capacitively-coupled radio-frequency $CF_4$ plasmas," J. Appl. Phys. **85**, 7562 (1999).

[16] O. V. Balachova, M. A. R. Alves, J. W. Swart, E. S. Braga, and L. Cescato, "$CF_4$ plasma etching of materials used in microelectronics manufacturing," Microelectron. J. **31**, 213 (2000).

[17] J. L. Mauer, J. S. Logan, L. B. Zielinski, and G. C. Schwartz, "Mechanism of silicon etching by $CF_4$ plasma," J. Vac. Sci. Technol. **15**, 1734 (1978).

[18] K. Suzuki, S. Okudaira, S. Nishimatsu, K. Usami, and I. Kanomata, "Microwave plasma etching of Si with CF4 and SF6 gas," J. Electrochem. Soc. **129**, 2764 (1982).

[19] Y. Cho, Y. Kim, S. Kim, and H. Chae, "Atomic layer etching of $SiO_2$ for surface cleaning using ammonium fluorosilicate with $CF_4/NH_3$ plasma," J. Vac. Sci. Technol. A **38**, 022604 (2020).

[20] V. O. Kuzmenko, A. V. Miakonkikh, and K. V. Rudenko, "Investigation of fluorocarbon film deposition from $Ar/CF_4/H$ plasma," High Energy Chem. **57**, S100 (2023).

[21] J. Nos, R. Dussart, T. Tillocher, P. Lefaucheux, and M. Boufnichel, "Evaluation of Bosch processing and $C_4F_8$ plasma deposition at cryogenic temperatures," J. Micromech. Microeng. **34**, 105011 (2024).

[22] C. B. Labelle, V. M. Donnelly, G. R. Bogart, R. L. Opila, and A. Kornblit, "Investigation of fluorocarbon plasma deposition from $c-C_4F_8$ for use as passivation during deep silicon etching," J. Vac. Sci. Technol. A **22**, 2500–2507 (2004).

[23] D. Zhang and M. J. Kushner, see https://cpseg.eecs.umich.edu/pub/presentations/dzhang_gec99.pdf for "Sticking coefficients of neutrals in an RF fluorocarbon discharge" (1999).

[24] M. Nagel, "Plasma-wall interaction in fluorocarbon plasmas," M.S. thesis (University of Greifswald, 2012).

[25] J. P. Booth, H. Abada, P. Chabert, and D. B. Graves, "CF $CF_2$ radical kinetics transport a pulsed $CF_4$ ICP," Plasma Sources Sci. Technol. **14**, 273 (2005).

[26] J. Luque, E. A. Hudson, and J.-P. Booth, "CF $A^2\Sigma+ – X^2\pi$ and $B^2\Delta – X^2\pi$ study by broadband absorption spectroscopy in a plasma etch reactor: Determination of transition probabilities, CF $X^2\pi$ concentrations, and gas temperatures," J. Chem Phys. **118**, 622 (2003).

[27] J.-P. Booth, "Optical and electrical diagnostics of fluorocarbon plasma etching processes," Plasma Sources Sci. Technol. **8**, 249 (1999).

[28] N. Bulcourt, J.-P. Booth, E. A. Hudson, J. Luque, D. K. W. Mok, E. P. Lee, F.-T. Chau, and J. M. Dyke, "Use of the ultraviolet absorption spectrum of CF2 to determine the spatially resolved absolute CF2 density, rotational temperature, and vibrational distribution in a plasma etching reactor," J. Chem. Phys. **120**, 9499 (2004).

[29] J.-P. Booth, G. Cunge, F. Neuilly, and N. Sadeghi, "Absolute radical densities in etching plasmas determined by broad-band UV absorption spectroscopy," Plasma Sources Sci. Technol. **7**, 423 (1998).

[30] Hamamatsu, see https://www.hamamatsu.com/content/dam/hamamatsu-photonics/sites/documents/99_SALES_LIBRARY/etd/LDLS_TLSZ1038E.pdf for "Laser-Driven Light Source LDLSTM" (2022).

[31] Princeton Instruments, see https://usermanual.wiki/Collections/Princeton-Instruments/public/manuals/Acton/SP-2750.pdf for "Operating Instructions Acton Series SP-2750" (2009).

[32] Teledyne Princeton Instruments, see https://www.teledynevisionsolutions.com/products/pylon/?model=PYL-400&vertical=tvs-princeton-instruments&segment=tvs for " PyLoN 400 Datasheet."

[33] S. Sharpe, B. Hartnett, H. S. Sethi, and D. Sethi, "Absorption cross-sections of $CF_2$ in the $\tilde{A}^1B_1$-$\tilde{X}^1A_1$ transition at 0.5 nm intervals and absolute rate constant for $2CF_2 \rightarrow C_2F_4$ at 298 ± 3K," J. Photochem. **38**, 1 (1987).

[34] G. Cunge, D. Vempaire, M. Touzeau, and N. Sadeghi, "Broadband and time-resolved absorption spectroscopy with light emitting diodes: Application to etching plasma monitoring," Appl. Phys. Lett. **91**, 231503 (2007).

[35] PubChem, see https://pubchem.ncbi.nlm.nih.gov/compound/Polytetrafluoroethylene "Polytetrafluoroethylene" (2023).

[36] Greenhouse Gas Protocol, see https://ghgprotocol.org/sites/default/files/2024-08/Global-Warming-Potential-Values (August 2024).pdf for "IPCC global warming potential values" (2024).

[37] P. Forster, T. Storelvmo, K. Armour *et al.*, Chapter 7: The Earth's energy budget, climate feedbacks and climate sensitivity, in *Climate Change 2021: The Physical Science Basis. Contribution of Working Group I to the Sixth Assessment Report of the Intergovernmental Panel on Climate Change* (Cambridge University Press, 2021), pp. 923–1054.